

Investigation of radiation damage due to particle irradiation on Silicon Drift Detector for Chandrayaan-2 mission

M. Shanmugam,^{a,1} S.V. Vadawale,^a A. Patel,^a S.K. Goyal,^a T. Ladiya,^a Y.B. Acharya,^a S. Pal^b and V. Nanal^b

^aPlanetary Sciences Division, Physical Research Laboratory,
Navrangpura, Ahmedabad, Gujarat, 380009 India

^bDepartment of Nuclear and Atomic Physics, Tata Institute of Fundamental Research,
Homi Bhabha Road, Colaba, Mumbai, 400005 India

E-mail: shansm@prl.res.in

ABSTRACT: This paper presents the work carried out in support of Silicon Drift Detector (SDD) characterization for the Chandrayaan-2 instruments namely Solar X-ray Monitor (XSM) and Alpha Particle X-ray Spectrometer (APXS). The XSM and APXS instruments use SDD to detect X-rays from the Sun and fluorescent X-rays from the lunar surface respectively. The aim of this study is to understand and quantify any spectroscopic performance degradation of these X-ray spectrometers due to space radiation in the SDD during its operational period. Any radiation damage to the SDD leads to increase in the detector leakage current and thus degrades the spectroscopic performance, mainly the energy resolution. The expected end-of-life (EOL) 10 MeV equivalent proton fluence was modeled using SPENVIS simulation software. The Silicon Drift Detector was irradiated with 10 MeV protons for the doses up to 24 krad in logarithmic steps and measured the energy resolution and the leakage current at each dose. The spectrometer energy resolution degraded from ~ 142 eV at 5.9 keV to ~ 250 eV for the cumulative proton dose of ~ 11 krad for the mission life of one year. This satisfies the performance requirement of the SDD based X-ray spectrometers onboard Chandrayaan-2 mission.

KEYWORDS: Radiation damage to detector materials (solid state); Spectrometers; X-ray detectors

¹Corresponding author.

Contents

1	Introduction	1
2	Space radiation environment and the proton dose	2
3	Radiation damage effects in Silicon detectors	3
3.1	Leakage current versus radiation damage	3
3.2	Temperature dependence of leakage current	4
4	Silicon Drift Detector based X-ray spectrometer	5
4.1	Silicon Drift Detector (SDD)	5
4.2	Design of X-ray spectrometer	5
5	Proton irradiation experimental setup and procedure	7
5.1	Experimental setup	7
5.2	Experimental procedure	7
6	Experimental results	9
6.1	Performance before proton irradiation	9
6.2	Performance after proton irradiation	11
6.2.1	Energy resolution	11
6.2.2	Leakage current	12
6.2.3	Leakage current versus energy resolution	13
6.3	Performance variation due to gamma versus proton radiation	13
7	Summary	14

1 Introduction

There are several scientific missions in the past decades that have carried Silicon Drift Detector (SDD) based X-ray spectrometers onboard [1]–[5] due to its superior spectroscopic performance in the low energy X-ray region. There are several missions planned in the near future with SDD based instruments onboard [6]–[8]. The spectroscopic performance, mainly the energy resolution of the Silicon detector based X-ray spectrometers onboard space/planetary missions degrade due to harsh environmental conditions such as temperature and radiation. The energy resolution of the silicon detector based X-ray spectrometer mainly depends on the detector leakage current and the readout electronics noise. The noise associated with the readout electronics is not expected to vary significantly during the mission life as the space instruments use radiation hardened space grade components. Hence, any degradation in the energy resolution is mainly due to the increase in the

leakage current. The leakage current in silicon detector varies with the operating temperature and the radiation damage in the space environment. The radiation damage in silicon detector is mainly due to displacement damage caused by the Non Ionizing Energy Loss (NEIL) of charged and neutral particles. This increases the leakage current and degrades the energy resolution. Performance measurements of various types of silicon detectors have been reported by irradiating the detectors with protons [9], gamma rays [10] and neutrons [11]. Proton irradiation measurements on the large area SDDs [12, 13] shows that the leakage current increases with proton dose. The change in the leakage current and the energy resolution due to X-ray and gamma ray radiation is reported in ref. [14]. These measurements show that the increase in the leakage current is due to the bulk damage in the silicon material and it is independent of type of the detector material [15].

Chandrayaan-2 mission is designed with an Orbiter, Lander named “Vikram” and a Rover named “Pragyan” having wide range of scientific experiments and launched on 22nd July, 2019. Two instruments onboard Chandrayaan-2 have SDD as a X-ray detector namely Solar X-ray Monitor (XSM) onboard orbiter and Alpha Particle X-ray Spectrometer (APXS) onboard rover. XSM experiment is aimed at measuring solar X-rays in the energy range of 1–15 keV around the Moon to estimate the global elemental composition of the Moon along with the companion instrument Chandra’s Large Area Soft x-ray Spectrometer (CLASS) which will measure the fluorescent X-rays from Moon surface. The SDD used in the APXS is expected to receive much lower proton dose as it is well shielded inside the lander craft during the launch condition and it has shorter operational life on the lunar surface due to extreme environmental conditions. To study the effect of proton induced radiation damage which is dominant during the transfer and in-orbit operations, we irradiated the SDD with protons of 10 MeV in logarithmic steps. At each step, the energy resolution and the leakage current is measured. Earlier we have investigated the effect of radiation on SDD performance by simulating the radiation environment using intense gamma radiation from ^{60}Co [14]. However, the gamma radiation does not completely simulate the NEIL of the radiation environment mainly consisting of high energy protons. In this context, we further investigated the space radiation damage effects on the SDD using protons.

In this paper, we report the change in the leakage current and the energy resolution measured for the proton doses up to 24 krad for various detector operating temperatures. The space radiation environment and the proton dose estimation is described in section 2 followed by radiation damage effects in silicon detector in section 3. Section 4 gives spectrometer design followed by proton irradiation experimental setup and procedure in section 5. The experimental results are discussed in section 6.

2 Space radiation environment and the proton dose

The SDDs onboard Chandrayaan-2 mission is expected to encounter highly energetic particles during the Earth to Moon transfer and Solar radiation on the Moon orbit. It is known that the Earth is surrounded by Van Allen radiation belts consisting of high energy electrons and protons trapped inside the Earth’s magnetosphere. The electron and proton flux in these regions can reach to $\sim 10^6$ electrons $\text{cm}^{-2} \text{s}^{-1}$ with maximum energy of 10 MeV and $\sim 10^5$ protons $\text{cm}^{-2} \text{s}^{-1}$ up to 400 MeV respectively. After launch, the Chandrayaan-2 space craft spent about 25 days around the Earth crossing the radiation belts multiple times. The spectroscopic performance of the SDD based

X-ray spectrometers are expected to degrade due to such intense space radiations and it is essential to quantify such variations for the mission of life of 1 year.

The particle fluence during the Earth to Moon transfer is estimated using Ap-8 proton model in the SPENVIS [16] (Space Environment Information System), a web based software suit developed by European Space Agency (ESA). The accumulated proton fluence during the transfer phase is estimated to $\sim 4.9 \times 10^{11}$ protons cm^{-2} in the energy range of 0.1 to 400 MeV. In the Moon orbit phase, for the mission life of 1 year, the SDD onboard Chandrayaan-2 orbiter will be exposed to solar protons which is the largest component of high energy proton exposure. The solar proton flux is estimated using JPL-91 solar fluence model with the confidence level of 95%. The model was run for the worst case scenario having the mission life of one year with solar maximum condition, gives the solar proton fluence of $\sim 4.8 \times 10^{11}$ protons cm^{-2} . The NIEL function in SPENVIS is used to estimate the equivalent fluence of 10 MeV protons considering the model incident proton spectra as well as total effective shielding. All the sides of the SDD in the XSM instrument is covered with Al metallic package having thickness of ~ 2 mm to protect the detector during the non-operating conditions which includes the radiation belts around the Earth. During the in orbit observations on the Moon, Solar X-rays will be detected through a small aperture having a diameter of ~ 0.7 mm in front of the detector. For 2 mm thick aluminum shielding, the trapped proton fluence reduces to $\sim 4 \times 10^8$ protons/ 40 mm^2 during the transfer orbits and to $\sim 5.5 \times 10^9$ protons/ 40 mm^2 during one year mission life in the lunar orbit as shown in figure 1. The contribution of solar proton induced radiation damage is ~ 10 times higher compared to trapped protons due to spectral hardness of solar protons, even though the total incident fluence of trapped and solar protons are same. The estimated equivalent radiation dose on the SDD is ~ 11 krad for the total proton fluence of $\sim 5.9 \times 10^9$ protons/ 40 mm^2 , considering the SDD mass of ~ 42 mg (active area of 40 mm^2 , 450 micron thick), for the mission life of 1 year.

3 Radiation damage effects in Silicon detectors

3.1 Leakage current versus radiation damage

Any radiation damage to the silicon detector results increase in the leakage current, poor charge collection efficiency and hence poor energy resolution. There are two types of radiation damage namely displacement damage and ionization damage [17]. The displacement damage is due to the non ionizing energy loss in the silicon bulk and the ionization damage is responsible for the surface leakage due to oxide layer interfaces. Both the processes contribute to the overall spectrometer performance degradation. The change in the leakage current due to radiation damage is given by the equation (3.1)

$$\Delta I_o = \alpha \Phi_{\text{eq}} V \quad (3.1)$$

where Φ_{eq} is the fluence of incident particles and V is the detector volume in which the leakage current is measured and α is the damage constant. The value of damage constant is of the order of 10^{-17} and shown to be varying with temperature [18, 19]. Researchers have also shown that the change in the leakage current is independent of type of silicon material. The radiation damage produced by different types of particles at various energies is usually compared with the particle fluence Φ_{eq} of the particular radiation to a reference value of 1 MeV neutrons by introducing a

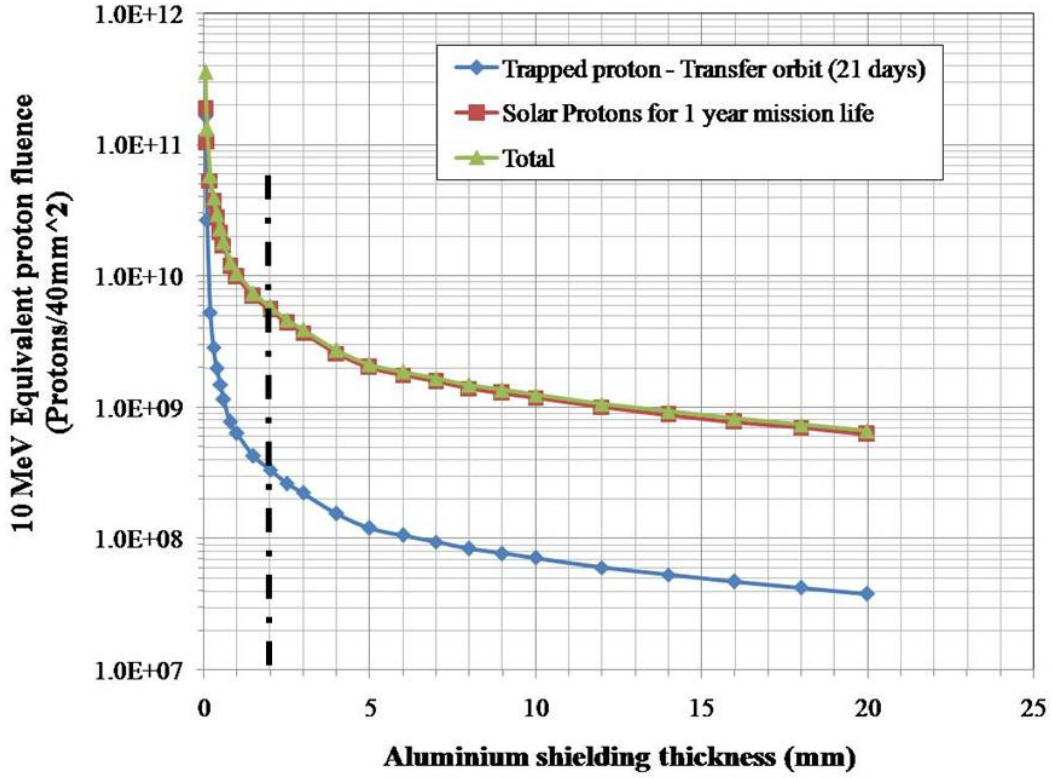


Figure 1. Estimated 10 MeV equivalent proton fluence for different aluminum shielding thickness.

harness factor κ [20] as given in the equation (3.2)

$$\Phi_{\text{eq}} = \kappa \Phi. \quad (3.2)$$

The value of the hardness factor based on the NIEL scaling hypothesis is the ratio of damage displacement function $\{D_i(E)\}$ for the particle (i) with energy (E) to the displacement damage function of 1 MeV neutrons (D_{neutron} for 1 MeV = 95 MeV mb). The value of hardness factor is one order magnitude higher in case of 1 MeV proton compared to 1 MeV neutron and in case of electron, it is two order magnitude lower [20].

3.2 Temperature dependence of leakage current

It is well known that the thermally generated charge carriers in the depleted bulk of the silicon detector is responsible for the change in the leakage current with the operating temperature. The leakage current exponentially varies with the temperature, which is given in (3.3)

$$I_o \propto T^2 e^{-E_g/2kT} \quad (3.3)$$

where I_o is the leakage current and T is the detector operating temperature, E_g is the band gap energy which is temperature dependent, and k is the Boltzmann's constant. The increase in the leakage current due to radiation damage has the same effect with temperature as that of non irradiated silicon detectors. In both these cases, the leakage current is originated from the thermal generation processes.

4 Silicon Drift Detector based X-ray spectrometer

4.1 Silicon Drift Detector (SDD)

In recent years, SDDs are the preferred choice for space based applications due to its superior spectroscopic performance in the low energy X-ray region. The working principle of SDD is based on the sideward depletion introduced by Gatti in 1984 [21]. SDD is functionally similar to Si PIN detector but has different electrode structure consisting of point anode at the center surrounded by a series of concentric annular rings with planar back contact. This architecture provides very low detector capacitance resulting in improved energy resolution and high count rate capability. SDDs planned onboard Chandrayaan-2 mission is procured from KETEK, GmbH which is available in the form of module. The SDD module consists of 450 micron thick SDD chip with active area of 30 mm^2 , JFET, feedback capacitor (f/b), reset diode, temperature sensor and the peltier cooler. The photographic view of the module is shown in figure 2.

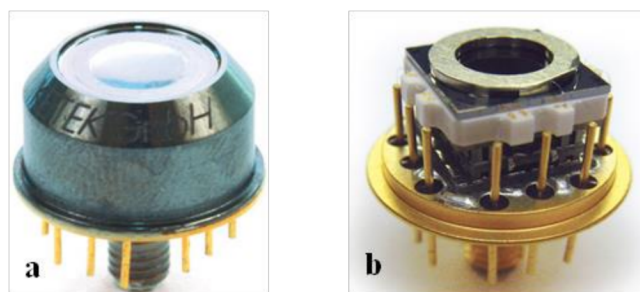


Figure 2. a) Photographic view of 40 mm^2 area SDD module, b) internal view (right) (Courtesy KETEK, GmbH).

4.2 Design of X-ray spectrometer

The spectrometer design consists of Front-End Electronics (FEE) and the Field Programmable Gate Array (FPGA) based back-end electronics. FEE is the analog pulse processing system consisting of Charge Sensitive Pre-Amplifier (CSPA) interfaced with SDD module followed by 5 pole CR-RC² based three stage shaping amplifier. The CSPA converts the charge into voltage pulses and the shaping amplifier converts the long tail CSPA output into semi-Gaussian shaped analog pulses with desired amplification. The output of the shaping amplifier is provided to peak detector to hold the peak signal amplitude and the Analog to Digital (A/D) converter converts the analog signal into digital form. The digital data from the A/D converter is then acquired by a FPGA based back-end electronics and converts into spectral form. The spectral data is then read by the LABVIEW based software in a computer via USB based serial interface. The detailed design is reported in ref. [22]. The photographic view of the developed spectrometer electronics is shown in figure 3.

The developed instrument provides the energy resolution of $\sim 142 \text{ eV}$ at 5.9 keV for the detector operating temperature of $\sim -35^\circ\text{C}$ and the pulse peaking time of $\sim 3 \mu\text{s}$. The SDD based X-ray spectrometer uses reset type CSPA. The output of reset type CSPA is in the form of ramp signal which is discharged through a reset pulse before it reaches the saturation level. The frequency of the reset pulse depends on the leakage current in the absence of any X-ray interacting with the detector.

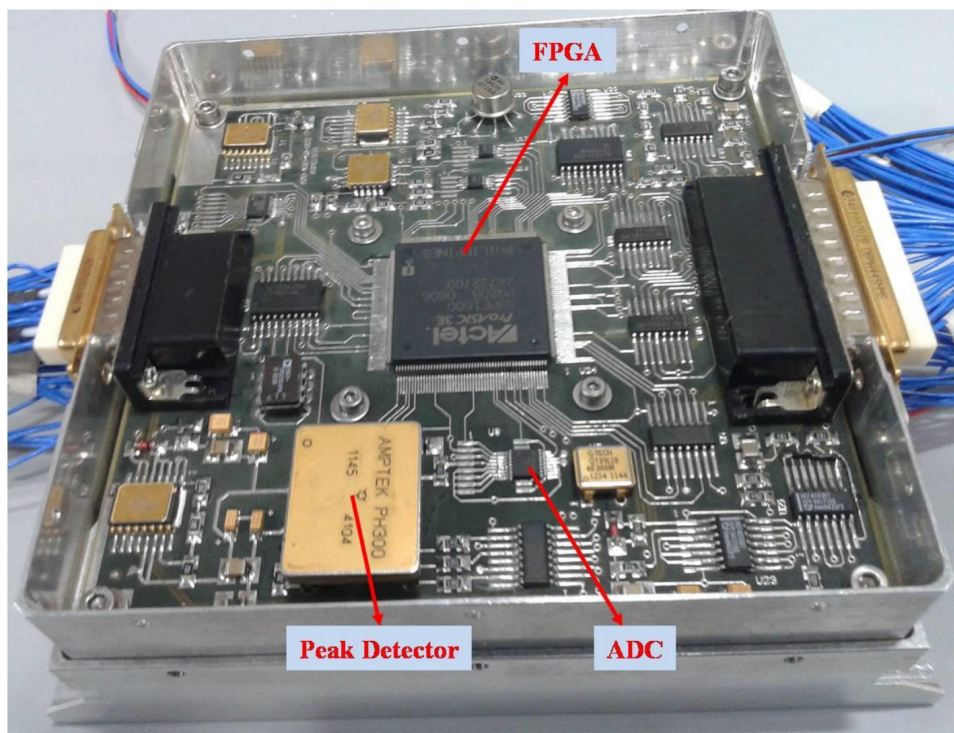
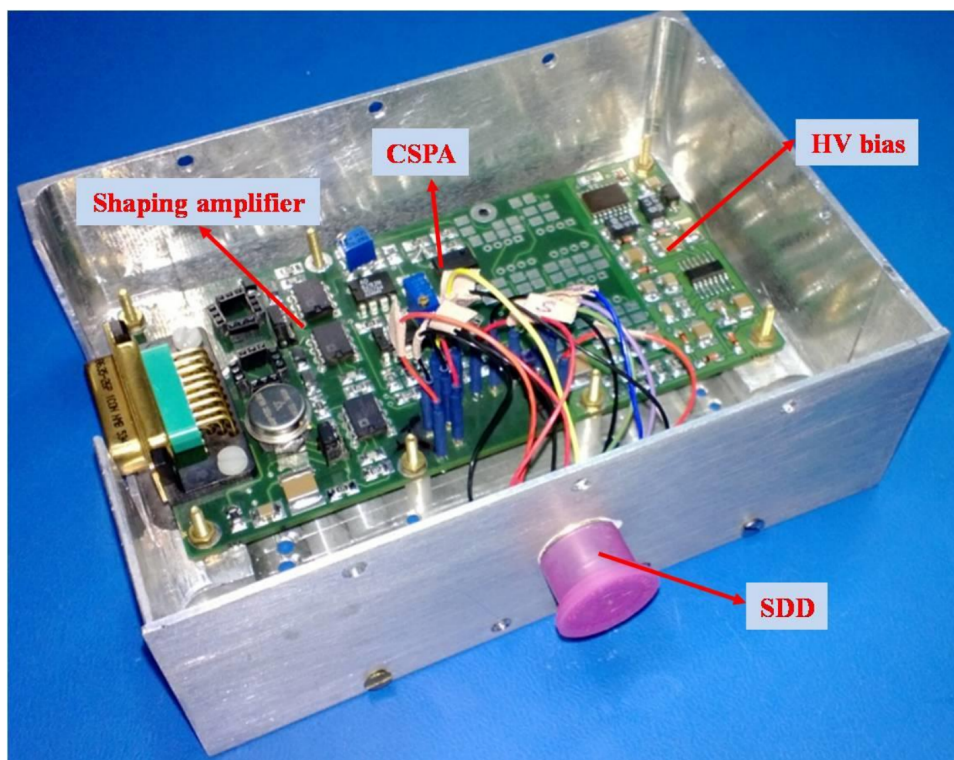


Figure 3. Photographic view of a) front-end electronics coupled with the SDD module, b) FPGA based back-end electronics.

So, one can estimate the leakage current from the SDD by counting the reset pulses without any additional hardware as described in ref. [22].

5 Proton irradiation experimental setup and procedure

5.1 Experimental setup

The experiment was carried out at the TIFR-BARC Pelletron facility, Mumbai, India using 10 MeV proton beam. Since the direct proton beam is extremely intense, hence the scattered protons are used for this irradiation experiment as shown in figure 4. The proton irradiation experiment setup consists of a vacuum chamber containing two movable platforms and an adjustable target holder. The SDD module with FEE was mounted on a movable platform at a distance of 20 cm from the target with scattering angle of 20 degree. A silicon detector based monitor was used to get the proton fluence and hence the radiation levels received by the SDD. The monitor detector was mounted at an scattering angle of 40 degrees. The target holder has a provision to mount multiple targets with varying foil thickness which can be changed during the course of the irradiation experiment as shown in figure 5. In our case, we mounted gold foils having thicknesses of 2.26 mg/cm^2 and 4.76 mg/cm^2 . We made a small enclosure to mount a Fe-55 radio-active source in one of the position on the target holder to characterize the SDD at each proton dose without breaking the vacuum environment.

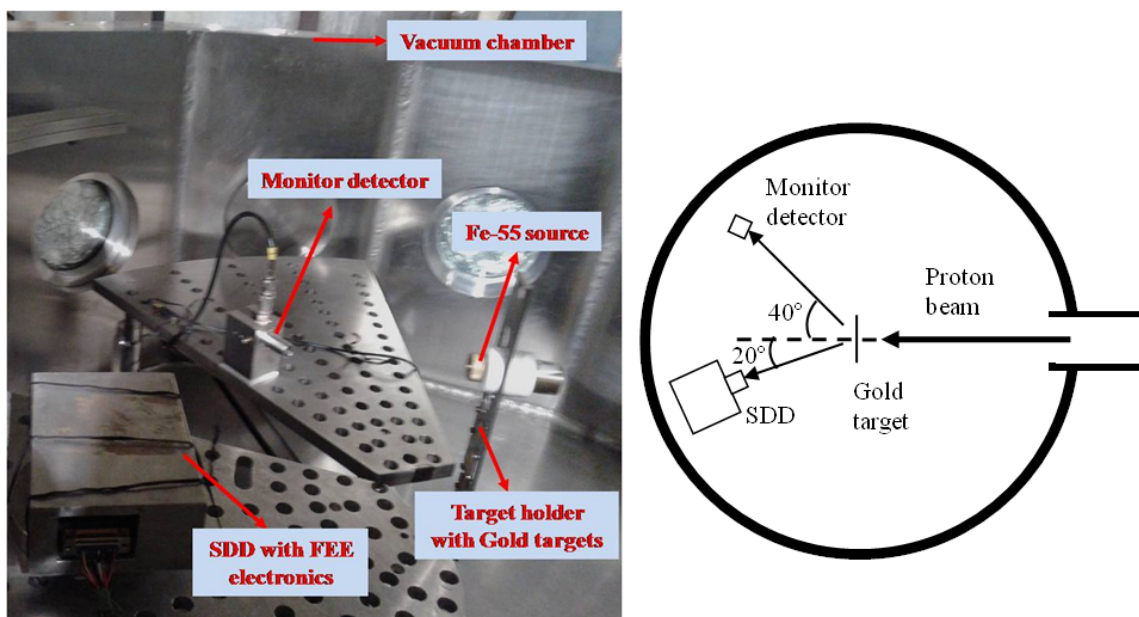


Figure 4. SDD proton irradiation experimental setup inside the vacuum chamber (left), Schematic representation of irradiation setup (right).

5.2 Experimental procedure

The proton irradiation experiment was carried by covering the SDD module with 2 mm thick aluminum enclosure all the sides having 3 mm diameter opening in the front side. This arrangement



Figure 5. Closer view of FEE with SDD module having 3 mm pin hole for proton irradiation (top) and the gold foil target holder with radiation active source for calibration (bottom).

protects the internal front-end JFET which is part of the SDD module from the radiation and exposes only the SDD chip to the incident protons as shown in figure 2. In this experiment, we employed thin gold sheets as scattering target. Each 10 MeV of scattered proton deposits ~ 5 MeV on the SDD bulk giving the dose of $\sim 1.9 \times 10^{-6}$ rads. The total proton radiation received by the SDD is estimated using the Rutherford scattering equation (4) and the proton counts registered in the monitor detector.

$$N(\theta) = \frac{N_i n L Z^2 k^2 e^4}{4r^2 K E^2 \sin^4(\theta/2)}. \quad (5.1)$$

Where N_i is the number of incident protons, n is atoms per unit volume, L is the thickness of target, Z is atomic number of the target, k is the Coulombs constant, e is the charge of the electron, r is the target to detector distance, KE is the kinetic energy of the proton and θ is the scattering angle. During the irradiation, the Pelletron beam current was set at around 5 nA for the doses up to 3 krad and increased to ~ 18 nA for the doses up to ~ 24 krad. The gold target having thickness of ~ 2.26 mg/cm² was kept in front of the beam for the doses up to 0.3 krad and target was changed to ~ 4.76 mg/cm² for the doses up ~ 24 krad. The dose estimated for SDD for various beam currents and the proton counts detected on the monitor detector are given in the table 1.

The proton doses were applied to the SDD in logarithmic scale and at each step, leakage current and the energy resolution was measured for various detector operating temperatures by stopping the beam line at each step. At the end of the beam line schedule, the monitor detector was positioned at various scattering angles. The proton counts received in the monitor detector was used to derive the angle dependent proton flux and also to compare with the estimated proton flux.

Table 1. Estimated cumulative proton dose on the SDD.

Run No.	Time (s)	Beam Current (nA)	Measured Integrated proton counts on Si Monitor detector	Estimated integrated total proton counts on SDD	Effective Dose (krad)	Cumulative Dose (krad)
1	900	5	182429	2745556	0.03	0.03
2	2160	5	431559	6494963	0.07	0.10
3	5100	5	1219856	18358833	0.20	0.30
4	6780	5	4245567	63895783	0.69	0.99
5	18900	5	12187578	183423049	1.98	2.97
6	29100	18	42504034	639685712	6.99	9.96
7	36300	18	87915977	1323135454	14.29	24.25

6 Experimental results

6.1 Performance before proton irradiation

The SDD based X-ray spectrometer performance has been characterized by measuring the leakage current and the energy resolution for various SDD operating temperatures in the laboratory environment. The spectrometer system provides the energy resolution of ~ 142 eV at 5.9 KeV for the pulse peaking time of ~ 3 μ s when the SDD is cooled to $\sim -35^\circ\text{C}$ as shown in figure 6.

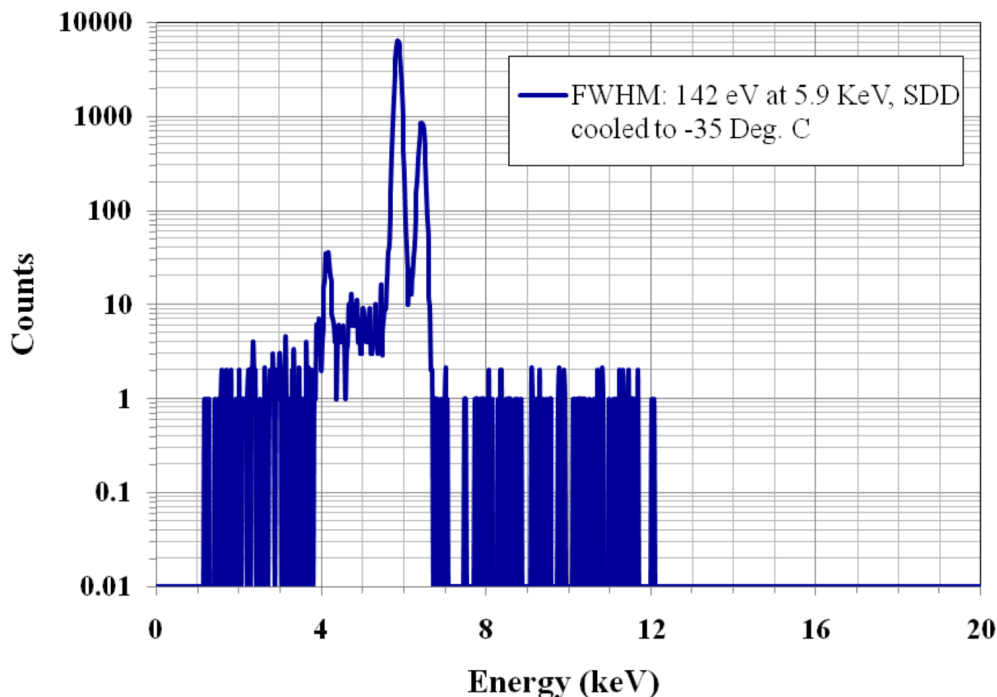


Figure 6. SDD based spectrometer energy resolution measured using Fe-55 X-ray source.

The energy resolution degrades from ~ 142 eV at -35°C to ~ 160 eV at -10°C and ~ 392 eV at 17°C for the 5.9 keV X-ray line as shown in figure 7. Cooling the SDD below -35°C does not

improve the energy resolution, even though the leakage current reduces to half. This is due the base line electronic noise which is dominant at lower detector operating temperatures and at higher detector operating temperatures, the leakage current determines the energy resolution.

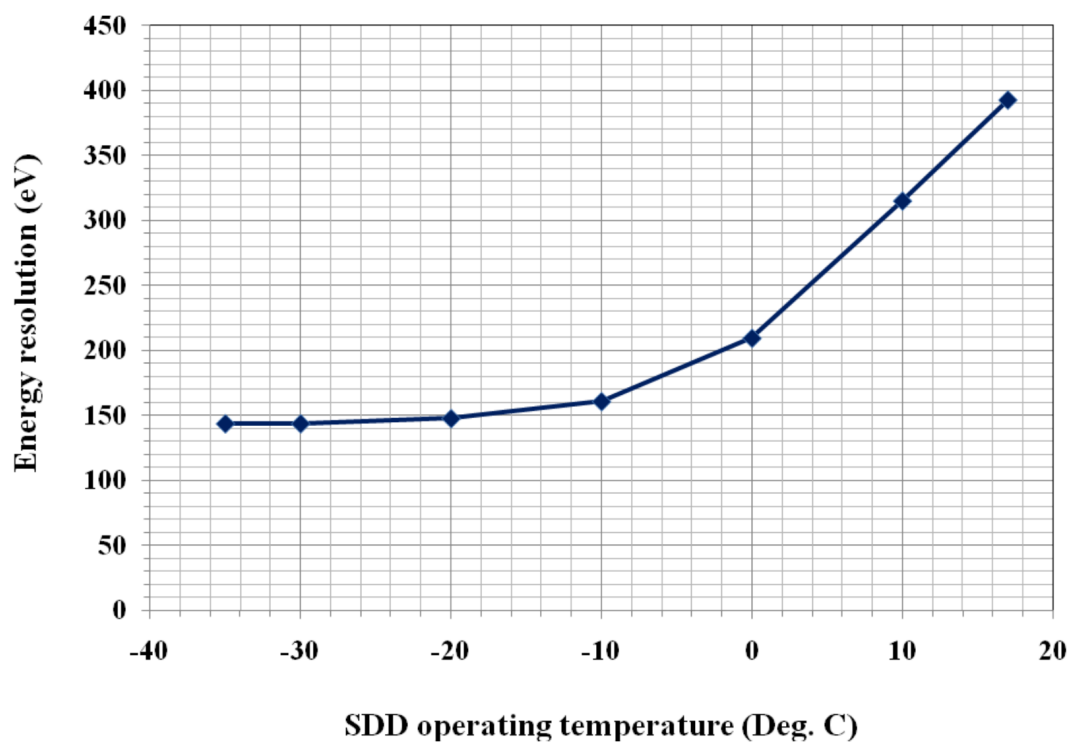


Figure 7. Energy resolution versus SDD module operating temperature in the laboratory environment.

The measured SDD leakage current is shown to be varying from ~ 0.1 pA for the detector operating temperature of $\sim -35^{\circ}\text{C}$ to ~ 100 pA at 17°C as shown in figure 9.

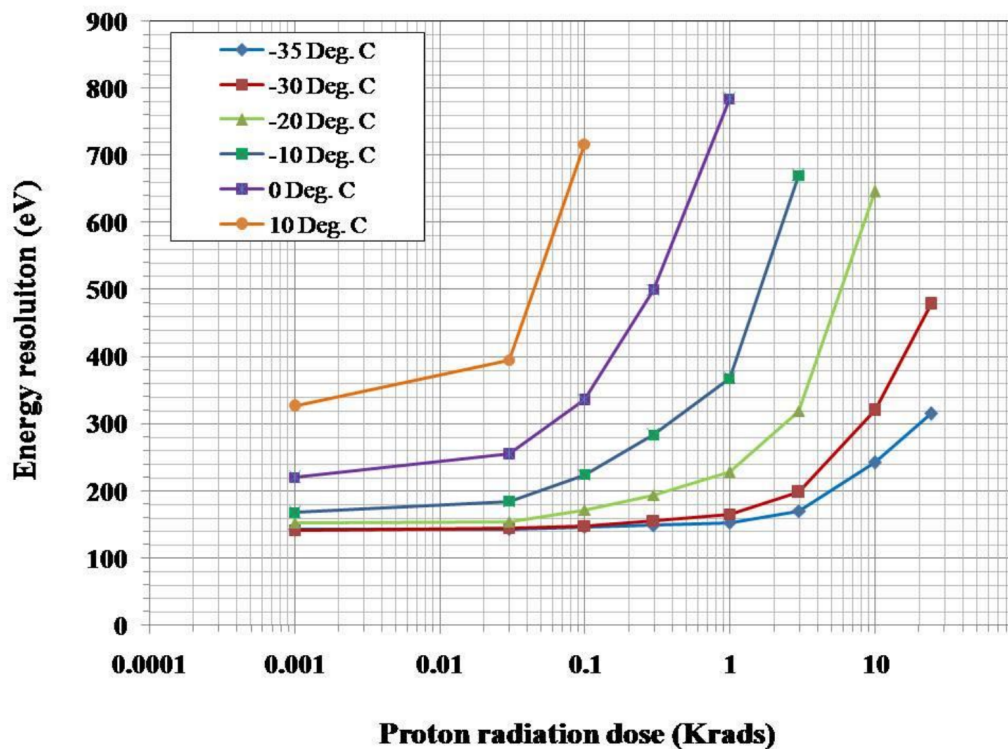


Figure 8. Energy resolution measured for various proton doses for different SDD operating temperatures.

6.2 Performance after proton irradiation

6.2.1 Energy resolution

The SDD chip was irradiated in logarithmic steps. The energy resolution and the leakage current were measured with SDD operating temperature in the range of -35°C to $+17^{\circ}\text{C}$. It is shown in figure 8 that the energy resolution degrades from $\sim 142\text{ eV}$ to $\sim 315\text{ eV}$ for the proton dose of $\sim 24\text{ krad}$ for the detector operating temperature of -35°C . Figure 8 also gives change in the energy resolution for proton doses from 0.1 rad up to 24 krad , for various detector operating temperatures. It can be clearly seen that the degradation in the energy resolution is much severe at higher detector operating temperatures. This confirms the fact that the radiation damage is sensitive to the detector operating temperature.

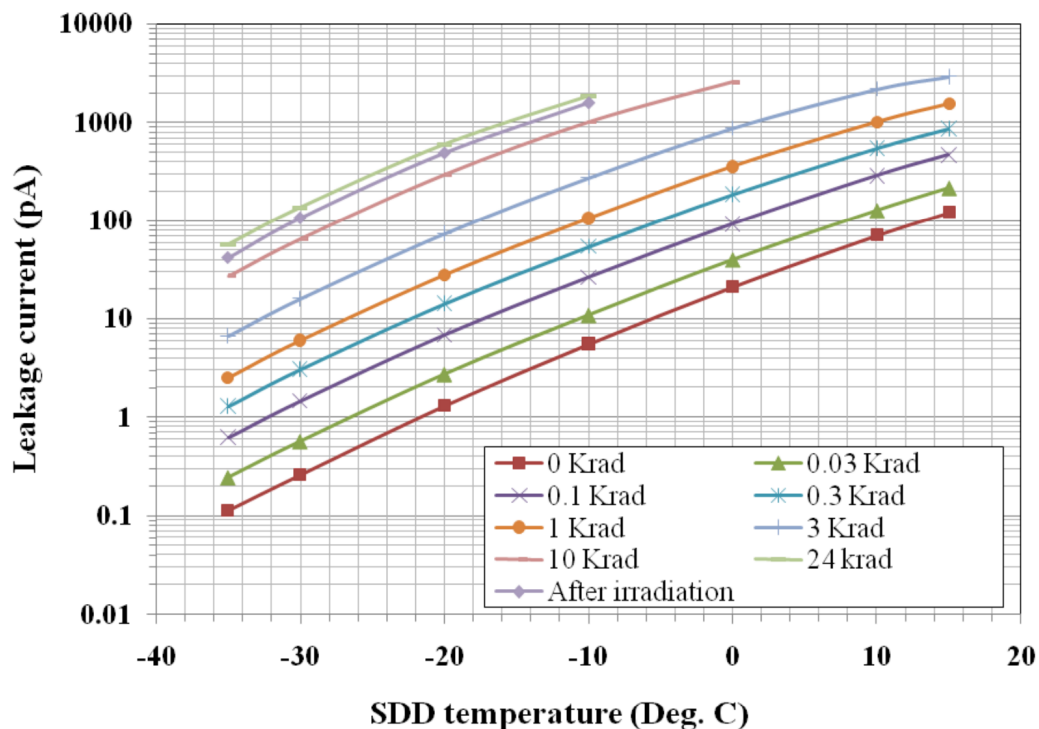


Figure 9. Leakage current measured for various SDD operating temperatures for different proton doses.

6.2.2 Leakage current

The increase in the SDD leakage current was also measured for each proton dose with temperature and it was observed that the leakage increases from ~ 0.1 pA to ~ 57 pA for the proton dose of 24 krad for the SDD operating temperature of -35°C . The change in the leakage current for various proton doses with temperature is shown in figure 9. It was found that the leakage current is decreased when measured few days after the irradiation. It could be due to annealing and subsequent measurement does not show any improvement when the system was stored in the ambient environment.

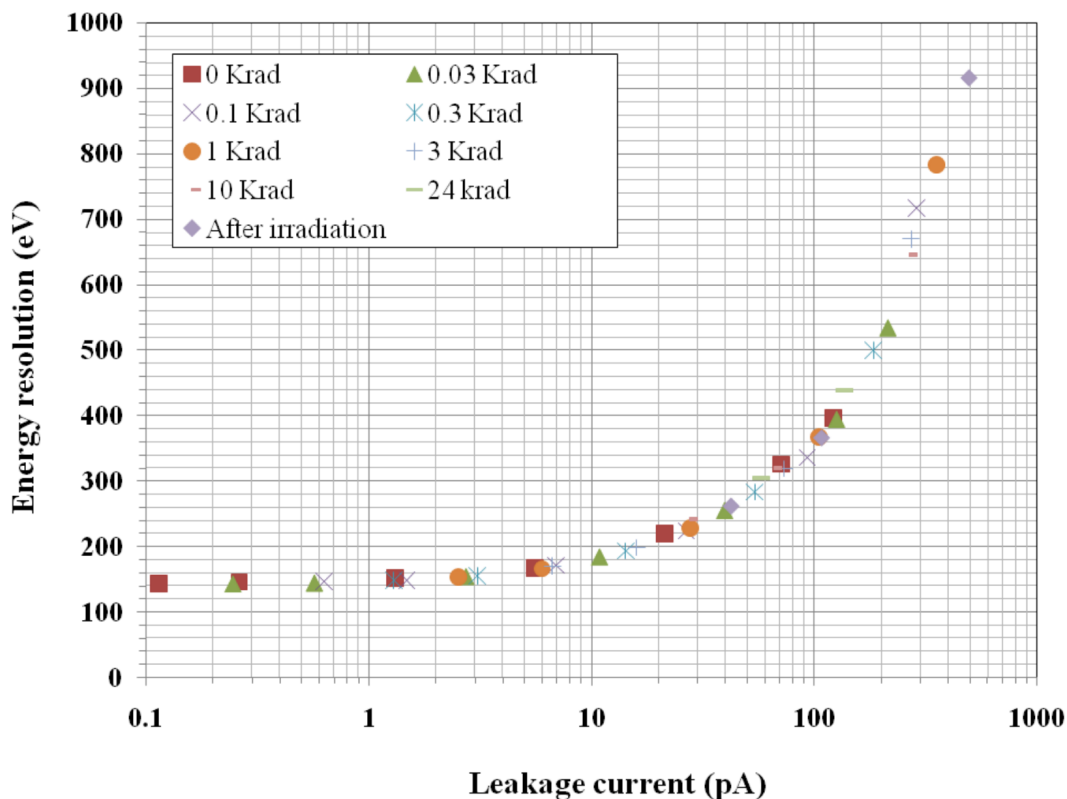


Figure 10. Measured value of leakage current plotted versus energy resolution for different proton doses.

6.2.3 Leakage current versus energy resolution

The measured value of leakage current for various detector operating temperatures are plotted with the measured energy resolution. It is shown in figure 10 that the energy resolution starts degrading for the detector leakage currents greater than 1 pA. The energy resolution degrades from ~ 142 eV for the detector leakage current of < 1 pA to 180 eV at 10 pA and 360 eV at 100 pA. It can be clearly seen that the energy resolution does not improve for the leakage currents < 1 pA. For the smaller leakage currents < 1 pA, the spectrometer system noise is dominant and hence the spectral energy resolution is constant at ~ 142 eV at 5.9 keV for the pulse peaking time of ~ 3 μ s.

Figure 10 gives consistent correlation between the leakage current and the energy resolution for various radiation doses. It is established that, one can estimate the performance degradation of the SDD based spectrometer due to radiation damage and it can be quantified by measuring the leakage current onboard.

6.3 Performance variation due to gamma versus proton radiation

In the earlier study [14], radiation damage effects on the SDD module was carried out using gamma rays for the doses up to 547 krad. It was shown that the energy resolution degrades to ~ 210 eV for the gamma ray dose of ~ 10 krad and to ~ 250 eV for 100 krad respectively. In this study, with proton irradiation, the energy resolution degrades to ~ 240 eV at 10 krad and to ~ 310 eV at 24 krad. The performance degradation of SDD based X-ray spectrometer due proton radiation gives the real

assessment of the instrument performance due to radiation damage as protons are the dominant radiation in the radiation belt around the Earth and Solar protons around the Moon.

7 Summary

The proton induced radiation damage and the performance degradation of the SDD based spectrometer have been studied. It is shown that the spectrometer energy resolution degrades from ~ 142 eV to ~ 250 eV for the proton dose of 11 krad. This meets the performance requirement of the SDD based X-ray spectrometers onboard Chandrayaan-2 for the mission life of 1 year. Further investigation reveals that the energy resolution degrades to ~ 315 eV for the dose of ~ 24 krad. These estimations are for the worst case scenario and we expect that any performance degradation will be within these limits. The change in the leakage current gives the measure of radiation damage on the SDD and the same has been demonstrated by measuring the energy resolution and the leakage current for various proton doses.

Acknowledgments

This research activity is carried out at Physical Research Laboratory (PRL) Ahmedabad, supported by Department of Space. The authors would like to thank TIFR-BARC Pelletron facility, Mumbai for the beam time and support.

References

- [1] R. Rieder et al., *The chemical composition of martian soil and rocks returned by the mobile Alpha Proton X-ray Spectrometer: Preliminary results from the X-ray mode*, *Science* **278** (1997) 1771.
- [2] R. Rieder et al., *The new Athena alpha particle X-ray spectrometer for the Mars exploration rovers*, *J. Geophys. Res. Planets* **108** (2003) 8066.
- [3] R. Gellert et al., *The Alpha-Particle-X-Ray-Spectrometer (APXS) for the Mars Science Laboratory (MSL) Rover Mission*, in proceedings of the *40th Lunar and Planetary Science Conference*, The Woodlands, Texas, U.S.A., 23–27 March 2009.
- [4] W.X. Peng et al., *Active Particle-Induced X-Ray Spectrometer for Chang’e-3 YuTu Rover Mission and its First Results*, in proceedings of the *45th Lunar and Planetary Science Conference*, The Woodlands, Texas, U.S.A., 17–21 March 2014.
- [5] C.K. Gendreau, *NICER Mission Overview, Status, and GO opportunities*, in proceedings of the *231th AAS Meeting*, National Harbor, Maryland, U.S.A., 8–12 January 2018.
- [6] M. Shanmugam et al., *Alpha Particle X-Ray Spectrometer (APXS) on-board Chandrayaan-2 rover*, in proceedings of the *42nd Lunar and Planetary Science Conference*, The Woodlands, Texas, U.S.A., 7–11 March 2011.
- [7] S. Vadawale et al., *Solar X-ray Monitor (XSM) on-board Chandrayaan-2 orbiter*, *Adv. Space Res.* **54** (2014) 2021.
- [8] S.N. Zhang et al., *eXTP: enhances X-ray Timing and Polarimetry Mission*, *Proc. SPIE* **9905** (2016) 99051Q.

- [9] R.S. Harper et al., *Evolution of silicon microstrip detector currents during proton irradiation at the CERN PS*, *Nucl. Instrum. Meth. A* **479** (2002) 548.
- [10] K. Hayashi et al., *Radiation effects on the silicon semiconductor detectors for the ASTRO-H mission*, *Nucl. Instrum. Meth. A* **699** (2013) 225.
- [11] H.W. Kraner, Z. Li and K.U. Posnecker, *Fast neutron damage in silicon detectors*, *Nucl. Instrum. Meth. A* **279** (1989) 266.
- [12] E. Del Monte et al., *Measurement of the effect of Non Ionising Energy Losses on the leakage current of Silicon Drift Detector prototypes for the LOFT satellite*, 2014 *JINST* **9** P07016 [[arXiv:1405.5466](https://arxiv.org/abs/1405.5466)].
- [13] E. Del Monte et al., *The effect of the displacement damage on the Charge Collection Efficiency in Silicon Drift Detectors for the LOFT satellite*, 2015 *JINST* **10** P05002 [[arXiv:1503.07682](https://arxiv.org/abs/1503.07682)].
- [14] M. Shanmugam, Y. Acharya, S. Vadawale and H. Mazumdar, *Radiation effects on Silicon Drift Detector based X-ray spectrometer on-board Chandrayaan-2 mission*, 2015 *JINST* **10** P09005.
- [15] CERN-ROSE/RD48 collaboration, *Leakage current of hadron irradiated silicon detectors — material dependence*, *Nucl. Instrum. Meth. A* **426** (1999) 87.
- [16] M. Kruglanski, E. de Donder and M. Neophytos, *Space Environment Information System (SPENVIS) in proceedings of the 38th COSPAR Scientific Assembly*, Bremen, Germany, 18–25 July 2010, volume 38, p. 4176.
- [17] V.A.J. Van Lint, *The Physics of Radiation Damage in Particle Detectors*, *Nucl. Instrum. Meth. A* **253** (1987) 453.
- [18] G. Segneri et al., *Measurement of the Current Related Damage Rate at -50°C and Consequences on Macropixel Detector Operation in Space Experiments*, *IEEE Trans. Nucl. Sci.* **56** (2009) 3734.
- [19] Z. Li et al., *Study of the long term stability of the effective concentration of ionized space charges (N_{eff}) of neutron irradiated silicon detectors fabricated by various thermal oxidation processes*, *IEEE Trans. Nucl. Sci.* **42** (1995) 219.
- [20] A. Vasilescu and G. Lindström, *Displacement damage in silicon*, (2000) <https://rd50.web.cern.ch/rd50/NIEL/default.html>.
- [21] E. Gatti and P. Rehak, *Semiconductor drift chamber — An application of a novel charge transport scheme*, *Nucl. Instrum. Meth.* **225** (1984) 608.
- [22] M. Shanmugam, Y.B. Acharya, S.V. Vadawale and H.S. Mazumdar, *A new technique for measuring the leakage current in Silicon Drift Detector based X-ray spectrometer — implications for on-board calibration*, 2015 *JINST* **10** P02009.